JCTC Journal of Chemical Theory and Computation

Confined But-2-ene Catalytic Isomerization Inside H-ZSM-5 Models: A DFT Study

Giampaolo Barone,[†] Nerina Armata,[†] Antonio Prestianni,[†] Teresa Rubino,[†] Dario Duca,*[,†] and Dmitry Yu. Murzin[‡]

Dipartimento di Chimica Inorganica e Analitica "S. Cannizzaro" dell'Università, viale delle Scienze Ed. 17, I-90128 Palermo, Italy, and Laboratory of Industrial Chemistry, Process Chemistry Centre, Åbo Akademi University, Biskopsgatan 8, FIN-20500 Åbo/Turku, Finland

Received September 25, 2008

Abstract: The isomerization of *cis*-but-2-ene to *trans*-but-2-ene within a 22T H-ZSM-5 zeolite model, also in the presence of two adsorbed Pd atoms, has been studied by DFT calculations. The results obtained allow us to state that the *cis*/*trans* but-2-ene isomerization can easily proceed inside unsupported zeolite cavities. In this case, differently than in the gas phase reaction, the *trans*-but-2-ene is less stable than the *cis*-but-2-ene, when adsorbed on the zeolite inner surface. Excluding the adsorption−desorption steps, the isomerization process involves two intermediates and three transition states, whose energy content is always very low with respect to that of reagents and intermediate species. The reaction is in principle allowed also in the presence of two Pd atoms embedded inside the zeolite cavity. However, strong H-Pd interactions seem to cause higher activation energies along the formation of the involved intermediates and transition states. To evaluate the confining effects of the zeolite room on the *cis*/*trans* isomerization process, the latter has been also analyzed on protonated (Pd_2H^+) and unprotonated (Pd_2) bare palladium fragments at different multiplicity states. The but-2-ene adsorption on the considered systems and the mutual influence occurring between the metal atoms and the hydrogen acidic sites at different multiplicity states have also been taken into consideration.

1. Introduction

Modeling of catalyzed processes is extensively employed to check and design reaction environments and mechanisms involved in heterogeneous catalytic systems.[1] Also the zeolite properties have been thoroughly investigated by computational approaches.[2,3]

Zeolite-based materials are extensively used in the catalytic hydrocarbon transformation, namely in cracking, hydrocracking, and C5−C7 isomerization.[4] The use of the acidic solid catalytic media, such as zeolite materials, with respect to the liquid ones, has indeed important technological and environmental implications related to selectivity, substrate separation, catalyst regeneration, large operating temperature ranges, absence of toxic byproduct formation, and, in general, facility of use, also avoiding waste production.[5] In particular, the ZSM-5 derived catalysts are used in fuel-cracking and isomerization as well as in methanol-to-gasoline conversion.[6]

Of course, the morphological and the chemical characteristics of the zeolite materials play an important role in the molecular surface adsorption and in the catalytic activity and selectivity.[7,8] In particular, the acidic properties caused by the substitution of Si^{4+} ions by couples of Al^{3+} and H^+ ions are fundamental in determining the local electrophilic character of the zeolite framework that is involved in driving the cation-promoted catalytic reactions in confined space.[9−11] In fact, the acidic Al-substituted zeolite locally provides a protonic environment to the adsorbed catalytic substrate (*Ad*), originating carbocation (carbonium and/or carbenium) intermediate (*In*), and transition state (TS) species,[12,13] which, mainly for the small olefin derivatives trapped inside the

* Corresponding author e-mail: dduca@cccp.unipa.it.
[†] Università di Palermo.
[‡] Åbo Akademi.

10.1021/ct800402k CCC: $40.75
Published on Web 04/21/2009

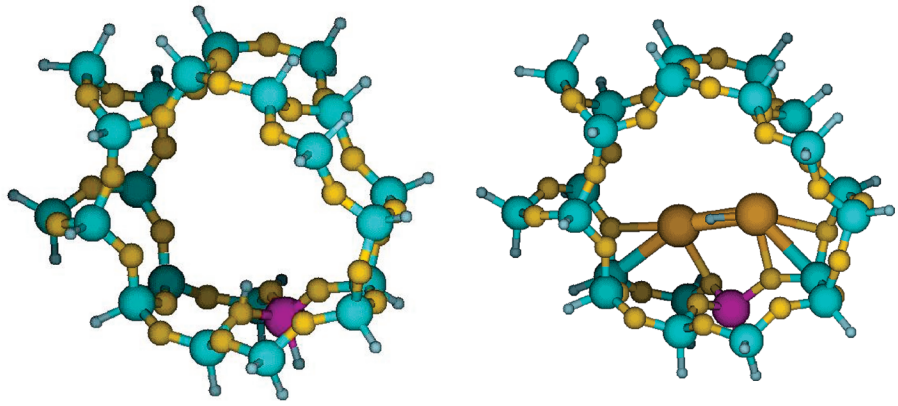

Figure 1. Singlet state HLBs optimized 22T H-ZSM-5 and Pd_2/H-ZSM-5 fragments employed in the kinetic study: H atoms, gray-blue; O atoms, gold; Si atoms, cyan; Al atom, purple; Pd atoms, brownish. The E_0 values for (a) and (b) are equal to −8598.7205 and −8852.2354 au.

zeolite cavities, are bulk-alkoxide and framework-anchored carbenium species.[14]

It is widely accepted that the computational chemistry has an enormous impact on the development of the zeolite catalytic materials and processes.[3] Focusing on the ZSM-5 systems, a few bibliographic examples of interest for the present work are reported in the following. Specifically, they concern i) reactivity,[13,15] ii) adsorption−desorption processes,[8,11] iii) proton transfer in the presence of metal centers,[16,17] and iv) Si/Al molar ratio effects and characterization of acidic sites.[18,19]

However, the employed models' sizes are not always adequate.[13,15,19,20] In this case, the lack of the zeolite cavity framework in studying the catalytic processes, hence the absence of local interactions between the catalytic substrate and the inner wall of the catalyst, generally causes an overestimation of the involved activation energy[21] and an unreliable estimate of the relative stability of molecules participating in a given reaction,[13] in particular, flattening the energetics of the involved zeolite systems.[19]

Macromolecular 22T H-ZSM-5 zeolite cluster models, also containing palladium centers, have been employed in the present work to study the *cis*/*trans* but-2-ene isomerization inside the zeolite cavity. Hydrogenation,[22] dehydrogenation, and double-bond migration[23] as well as oligomerization of the butene molecules[24] or skeletal transformations that involve the 2-methylpropene formation[25] were not considered, being beyond the scope of the present work. In fact, the *cis*/*trans* title isomerization is rooted in pioneering works on photo- and iodine-catalyzed *cis*- to *trans*-but-2-ene isomerization,[26] and it is up till now considered as an introductory example in understanding the basic principles of catalysis.[27,28] The choice of studying the *cis*/*trans* isomerization process inside the zeolite cavity in the presence of small metal clusters is conversely desirable because isomerization catalysts (e.g., metals) and shape selective materials (e.g., zeolites), taken together, can be effective in butene double bond migration/isomerization processes of practical interest.[29]

This paper, referring to uncatalyzed as well as to bare-palladium catalyzed processes, examines the confinement effects of the H-ZSM-5 zeolite cavity and the influence of embedded palladium atoms on the proton-activated *cis*/*trans* but-2-ene isomerization. Electronic charge transfers involved in the isomerization processes inside the zeolite cavity embedding or not the palladium atoms are also qualitatively investigated.

The paper organization is explained as follows. In section 2, the properties of the models employed are given with the essential features characterizing the computational methods. In section 3, details on the structural and mechanistic findings are presented, discussing the following: the metal effects on the zeolite Brønsted acidity sites (*BASs*) (section 3.1); the but-2-ene adsorption on zeolite fragments (section 3.2); the uncatalyzed but-2-ene isomerization (section 3.3); and the catalyzed but-2-ene isomerization on the zeolite fragments (section 3.4). Supporting Information is available and concerns the following: the influence of different basis sets employed to study the title reaction; the aggregation sites of the palladium atoms inside the zeolite cavity; and the multiplicity states of the supported systems.

2. Computational Details

Structural and kinetic properties of but-2-ene derivatives, both isolated and within a 22T H-ZSM-5 zeolite model, were calculated. The 22T H-ZSM-5 system, also supporting palladium atoms (Pd_2/H-ZSM-5), consists of two 10T rings connected by two T moieties (see Figure 1). Reference calculations on the same hydrocarbons, interacting with bare palladium fragments, both protonated (Pd_2H^+) or not (Pd_2), were also performed. Different multiplicity states were taken into consideration either for the bare-palladium or for the supported zeolite systems. The zeolite cavity chosen is a model of the largest pore present in a ZSM-5 zeolite. As recently reported for a very similar reaction system,[15] the cluster approach has been employed.[30] The starting zeolite model (ZSM-5), whose coordinates were taken from a DLS refined X-ray structure,[31] consists of 81 atoms of which 28 cutoff (capping) hydrogens, bound to silicon atoms, substitute the original oxygens to truncate the periodic zeolite structure. In order to mimic the acidic zeolite system (H-ZSM-5), one

silicon was substituted by one aluminum atom whereas one hydrogen atom was bound to a T_4OT_1 position,[32] through an oxygen site vicinal to the aluminum and pointing within the zeolite cavity[19] (see Figure 1a). This hydrogen acidic site corresponds to one of the more stable *BASs* in the largest zeolite H-ZSM-5 10T ring,[19] and for this reason it has been selected to mimic a possible catalytic site within a zeolite cavity.

The calculations were performed using the Gaussian03[33] program package, by optimizing the different geometries at the DFT B3LYP[34] level. This choice was supported by the results reported by Tirado-Rives and Jorgensen,[35] which showed that this DFT functional is very effective in estimating the isomerization of several organic molecules. Time-dependent[36] and unrestricted[37] DFT calculations were performed on the species involved in the *cis*/*trans* uncatalyzed isomerization.

Two different groups of basis sets, in the following indicated as low level basis sets (LLBs) and high level basis sets (HLBs), were mainly employed for the calculations. The LLBs procedure makes use of i) the 6-31G(d,p)[38] basis set for the atoms of the but-2-ene derivatives involved in the catalyzed reactions (section 3.4) and for the Al, O, and the acidic H atoms of the aluminum-modified T environment, ii) the 3-21G[39] basis set for the Si, O, and H atoms of the remaining 21T fragments, and iii) the LANL2DZ[40] basis set for the Pd atoms. The HLBs approach differs from the LLBs one due to the use of the 6-31G(d,p) basis sets for the silicon and oxygen atoms belonging to the 21T moieties of the zeolite rings.

The uncatalyzed (section 3.3) and the bare-palladium catalyzed (section 3.4.2) reactions were investigated by the HLBs. The geometries at the energy minima were optimized by employing both HLBs and LLBs. Moreover, single point calculations (SP_{df}) were performed on structures optimized by using the HLBs and employing the 6-311+G(2d,2p)[41] instead of the 6-31G(d,p) basis set. The LLBs was chosen to limit the computational time with the hypothesis that the differential energetics and the local properties of the treated zeolite systems could be described with adequate accuracy even with a small basis set. The HLBs and the SP_{df} approaches were conversely employed to test the reliability of the hypothesis above.

Vibration analysis within the harmonic approximation of the energy minimum structures was performed[42] on all the optimized geometries. Due to the fact that the geometry of the investigated models was partially optimized, fixing the coordinates of the cutoff external hydrogens, 29−31 spurious imaginary frequencies were always observed, essentially identical in all the systems. This suggests that an error cancelation should occur when considering relative values of the calculated standard free energy and enthalpy at a given temperature. Both the thermochemical parameters above were calculated at 298.15 K to study the acidic properties of the considered H-ZSM-5 systems, after the zero-point energy correction,[42] always in the frame of the mentioned harmonic approximation of the vibrational potential. Transition states, calculated by the LLBs approach, were fixed by the synchronous transit-guided quasi-Newton method.[43] Noticeably, during the vibration analysis of the TSs, it was always possible to find one imaginary frequency attributable to a corresponding reaction coordinate.[42] As a consequence, we have been able to discriminate among energy-minimum and saddle-point constrained geometries. Finally, in the evaluation of the adsorption energies, characterizing the interaction of the hydrocarbon and the 22T fragments, the BSSE correction[44] was always introduced, namely for the SP_{df}, HLBs, and LLBs systems.

Scheme 1. Details on the *cis*/*trans*-But-2-ene Isomerization Pathway

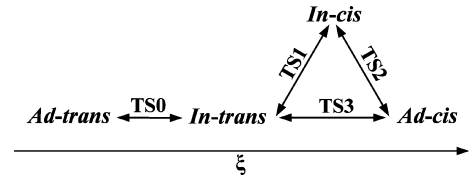

Starting from the X-ray coordinates of the ZSM-5 model, partial geometry optimizations were initially performed on the 28 external cutoff hydrogen atoms; subsequently, by fixing the coordinates of the external hydrogen atoms, the partial optimization was extended to the remaining atoms of the 22T unsupported (H-ZSM-5) and supported (Pd_2/H-ZSM-5) models. Figure 1 shows the optimized geometries of H-ZSM-5 and Pd_2/H-ZSM-5, being the corresponding structures obtained by HLBs and LLBs indistinguishable by sight.

3. Results and Discussion

The calculated *cis*/*trans* but-2-ene isomerization pathway, occurring inside the H-ZSM-5 zeolite cavities, is shown in Scheme 1. The reaction-coordinate (ξ) connects the least to the most stable but-2-ene isomer found inside the zeolite fragments, namely the *trans*-but-2-ene to the *cis*-but-2-ene (see section 3.4). *Ad-cis* and *Ad-trans* represent the corresponding but-2-ene adsorbed species, while *In-cis* and *In-trans* represent the intermediate conformer species geometrically more similar to the *Ad-cis* and *Ad-trans*, respectively. Finally, TS0-TS3 are the transition states along the catalytic isomerization pathway, with TS3 obtained only for the unsupported zeolite model. It is worth pointing out that both structures and energies of TS2 and TS3 were essentially coincident.

The reaction mechanism sketched in Scheme 1 is only a portion of the whole catalytic butene transformation process that also implicates by side surface reactions[22−26] as well as adsorption, desorption, and diffusion of the involved species. In the present paper we have focused on the effects of the zeolite confinement and on the influence of embedded palladium atoms on the reaction steps, leading from *cis*- to *trans*-but-2-ene and *vice versa*. The nonactivated adsorption energy (E_{ad}) values of the *cis* and *trans* species are discussed in section 3.2.

3.1. Metal Effects on the H-ZSM-5 Acidity. A preliminary study (see the Supporting Information) points out that the catalytic activity of the bifunctional palladium supported H-ZSM-5 systems toward the hydrogen-induced reactivity of light unsaturated hydrocarbons could be mainly attributed

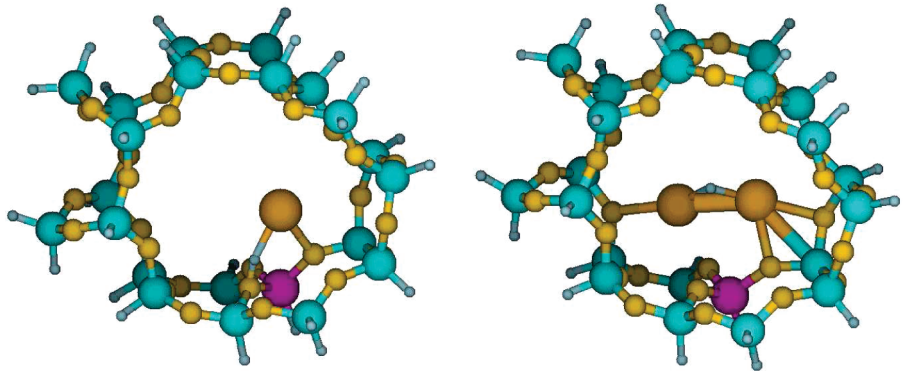

(a) (b)

Figure 2. Palladium supported systems: (a) singlet ground-state HLBs optimized 22T Pd/H-ZSM-5 fragment: $E_0 = -8725.4620$ au and (b) triplet ground-state HLBs optimized 22T Pd_2/H-ZSM-5 fragment: $E_0 = -8852.2354$ au.

Table 1. Deprotonation of Different H-ZSM-5 Fragments: Values of Energy and Standard Free Energy at 298.15 K Calculated at the Ground States by the LLBs and HLBs Approaches

	LLBs		HLBs	
fragment[a]	ΔE/kJ/mol	$\Delta G°$/kJ/mol	ΔE/kJ/mol	$\Delta G°$/kJ/mol
H-ZSM-5	1278	1252	1254	1224
Pd/H-ZSM-5	1297	1272	1277	1250
Pd_2/H-ZSM-5	1448	1419	1378	1362

[a] Both protonated and nonprotonated H-ZSM-5 and Pd/H-ZSM-5 fragments showed singlet ground states, whereas the Pd_2/H-ZSM-5 fragment was at triplet and singlet state in the protonated and nonprotonated forms, respectively.

to the availability of (ionic or atomic) hydrogens -- either derived from *BASs* and/or produced by external sources -- interacting with small palladium fragments adsorbed nearby the aluminum-modified T fragments.

Several palladium supported fragments have been considered (see the Supporting Information) with the general formula Pd_n/H-ZSM-5 (with $n = 1-2$). The analysis of the most stable systems found points out that the acidic hydrogens near the aluminum atom represent the favorite nucleation centers for the deposition of palladium atoms, see Figures 1b and 2. This result induced us to evaluate the relative acidity of the most stable Pd_n/H-ZSM-5 model systems, presuming that local acidity changes caused by the palladium atoms embedded in the zeolite framework could affect the catalytic activity. The increased stability of the metal supported systems is indeed an interesting issue related to the decrease of the zeolite acidity strength, detected experimentally in the presence of adsorbed Group 10 metal crystallites.[45]

The acidity strength was estimated by calculating the values of deprotonation energy[10] and standard free energy at 298.15 K. Table 1 shows the results concerning the unsupported and supported fragments: H-ZSM-5, Pd/H-ZSM-5, and Pd_2/H-ZSM-5. The energy and standard free energies, irrespective of the basis set level, show that the strong acidity of the zeolite is decreased by the presence of also low metal content, in agreement with the experiment.[45] Noticeably, the deprotonation energy values of the nonsupported fragment calculated by the LLBs and HLBs procedures are in good agreement (ca. 5% and 3% of difference, respectively) with the analogous parameter calculated for H-ferrierite by Nieminen et al.[10]

The decrease of the acidity of the H-ZSM-5 fragments with the increase of the number of adsorbed Pd atoms can be ascribed to hydrogen migration from the support to the embedded metal atoms. Hence, the acidity, if referred to the mobility of H from the -OH acidic group, is locally increased by the metal atoms that, however, fix the same hydrogen, producing at a macroscopic level an apparently lower acidity. There is indeed a strong affinity between the H species and the Pd_2 fragment, such that the character of the former changes from acidic to hydride-like. This behavior is supported by a Mulliken population analysis (not shown), from which electron deficency on the metal atoms can be deduced, in agreement with experimental findings.[45]

On the whole, our results nicely explain the modified acidic properties of the bifunctional zeolite derivatives, whose experimental catalytic properties already seemed to be affected by the mutual interaction of the metallic and acidic functions.[45] This further justifies the choice to investigate the influence of the palladium atoms in the but-2-ene isomerization inside the H-ZSM-5 fragment. As already mentioned, the Pd_2/H-ZSM-5 system was employed for this purpose. Since this one as well as the smaller reference systems -- Pd_2 and Pd_2H^+ -- showed singlet ground state when interacting with hydrocarbon derivatives (see section 3.4.2), the kinetic study was followed just in the singlet state. Moreover, due to the close similitude found, by applying the HLBs and LLBs approaches, on the geometrical and the energetic parameters of both the supported and the nonsupported H-ZSM-5 catalyst models (see the Supporting Information), we decided to detail the title kinetic study by the less time-consuming method, namely the LLBs one.

3.2. But-2-ene Adsorption on the H-ZSM-5 Fragments. In Table 2 the BSSE corrected adsorption energy of *cis*-but-2-ene and *trans*-but-2-ene on the H-ZSM-5 22T fragments embedding or not palladium atoms is reported, using different basis sets. It is also reported the coefficient of variation calculated for the counterpoise BSSE corrections corresponding to the energy minimum species involved in the reaction paths of Scheme 1. The unsupported H-ZSM-5 systems showed that the but-2-ene adsorptions on the T_4OT_1 site[15] occur via π interactions. The LLBs and HLBs adsorp-

Table 2. BSSE Corrected Ground-State Adsorption Energy of *cis*-But-2-ene and *trans*-But-2-ene on H-ZSM-5 22T Fragments without and with Palladium, Using Different Basis Sets

approach level	Ead_{cis}[a]/kJ/mol	Ead_{trans}[a]/kJ/mol	vc[a,b]
LLBs	22.3 | 190.3	13.2 | 182.2	0.003 | 0.036
HLBs	14.5 | 162.5	4.7 | 141.2	0.046 | 0.012
SP_{df}	12.6 | 200.2	3.4 | 167.8	0.055 | 0.012

[a] On the left and on the right, the values of the unsupported and supported systems are reported, respectively. As the H-ZSM-5 system, both the adsorbed fragments were in singlet ground state, while the Pd_2/H-ZSM-5 ground state was a triplet. [b] Coefficient of variation -- $vc = (\sigma)/(\mu)$, with σ and μ being the standard deviation and the mean values calculated for the counterpoise BSSE correction values, respectively. These are determined by a given basis set, for all the energy minimum species involved in the reaction paths of Scheme 1.

tion energies are in the range of those calculated for larger 52T H-ZSM-5 fragments by DFT B3LYP cluster approaches.[19]

An inversion of the stability order between *cis* and *trans* adsorbed species is observed, both for the embedding and nonembedding palladium atoms fragment and irrespective of the basis set considered. This result, which is in agreement with the activation energies characterizing the diffusion of the same but-2-ene isomers in analogous unsupported zeolite systems,[46] could be explained considering the constraining effects of the zeolite cavity[10,19,46] and in particular the lower steric repulsion felt by the *cis*-but-2-ene isomer within the 10T zeolite cavity. For the unsupported systems a characteristic decreasing trend of the adsorption energies, with the increasing of the basis set size, is clear. The same trend is conversely not observed for the Pd supported fragments.

In fact, it has not been yet possible to determine the experimental adsorption energies of these systems,[46] and in a recent study on the 2-methylpropene on unsupported H-ferrierite, Tuma and Sauer turned to the consideration of the corresponding saturated hydrocarbon adsorption energies in order to have experimental references.[11] The adsorption energies obtained by those authors using a hybrid MP2:DFT approach accounting for the dispersion effects occurring inside the zeolite cavity showed even higher values than the experimental references. Analogous results were reported for similar systems, using QM/MM methods[10] designed to include dispersion effects.

The adsorption energy values of Table 2 are smaller than those obtained by approaches specifically designed to include dispersion effects[10,11] while, as a paradox, becoming even smaller increasing the calculation level, up to include diffuse functions in the DFT B3LYP treatments. On the other hand, the results reported in Table 2 are in good agreement with DFT periodic calculations performed at a comparable level.[11] However, it can be also considered that the difficulties to perform experimental measurements of the π adsorbed hydrocarbons on -OH groups of acidic zeolites might be a consequence of the high reactivity of the resulting adduct.[46]

Whereupon, in our opinion, it is not straightforward to conclude that zeolite cavities containing highly reactive unsaturated hydrocarbons must show either higher or lower local energies, compared to those zeolite cavities containing less reactive saturated hydrocarbons. In any case, the values of the *vc* parameter reported in Table 2 clearly show that the variations on the average BSSE correction value with respect to a given basis set are very small irrespective of the involved zeolite system (i.e., supported or nonsupported). As a consequence, in agreement with the recent works of Gleeson[15] and Tirado-Rives and Jorgensen,[35] it is reasonable to consider that the results of the energetic differential approach to the study of the title isomerization -- and in particular of the steric pressure exerted by the cavity on the reaction species -- has to be considered consistent also when using the LLBs.

Furthermore, it is to be observed that the singlet ground-state HLBs di-σ adsorption energy of the *cis*-but-2-ene resulted 202.0 and 115.0 kJ/mol on the bare Pd_2H^+ and Pd_2 fragments, whereas in the same order on the same fragments the di-σ adsorption energy was 199.0 and 117.6 kJ/mol for the *trans*-but-2-ene. The unprotonated and the protonated Pd_2 bare fragments showed singlet and triplet ground states, whereas the di-σ adsorption mode, in agreement with Delbecq and Zaera,[28] always resulted in being more stable than the π mode in the ground state, irrespective of the considered but-2-ene isomer. Finally the relative stabilization of the *cis* species with respect to the *trans* one in the Pd_2H^+ systems is stressed.

Comparing these findings with those summarized in the row 6-31G(d,p) of Table 2, it is straightforward to recognize the role, in the but-2-ene adsorption processes, of both the acidic center (stabilizing) and of the zeolite cavity (destabilizing). Of course, these properties will affect catalytic reactivity and selectivity of the zeolite material.

3.3. Uncatalyzed But-2-ene Isomerization. The *in vacuo* *cis*/*trans* but-2-ene isomerization should involve i) the C2-C3 lengthening (double-bond breaking), ii) the rotation of 180° around the C2-C3 bond, and iii) the C2-C3 double-bond back-formation. Similar transformations characterize the rotation around the double bond of ethylene. Post HF calculations revealed the existence of a possible photochemical mechanism in which the TS of ethylene, showing a 90° rotation around the C-C double bond, would be a degenerate singlet−triplet spin state, $^1(\pi\pi^*)$ and $^3(\pi\pi^*)$ respectively, characterized by a relative energy of ca. 300 kJ/mol higher than the ground state.[47]

By using unrestricted DFT calculations,[37] we found a $^3(\pi\pi^*)$ state with the C2-C3 rotated by 90° that can be identified as the TS species in the gas phase *cis*/*trans* isomerization. This species shows an energy value 260 kJ/mol higher than that of the most stable isomer (*trans*-but-2-ene). The value is in good agreement with the one reported for ethylene and also with the experimental value found in the gas phase *cis*/*trans* isomerization (264 kJ/mol).[27] Further calculations on the uncatalyzed systems showed that i) the *trans*- and *cis*-but-2-ene ground state differ by ca. 5 kJ/mol, being the first more stable, ii) the Franck−Condon $\pi^2 \rightarrow {}^1(\pi\pi^*)$ *trans*-but-2-ene transition energy determined at the TD-DFT level[36] is equal to 737 kJ/mol, in excellent agreement with the value found for the ethylene system (800 kJ/mol),[47] and iii) both the unrotated *cis*- and *trans*-but-2-ene $^1(\pi\pi^*)$ states are less stable than the unrotated *trans*-

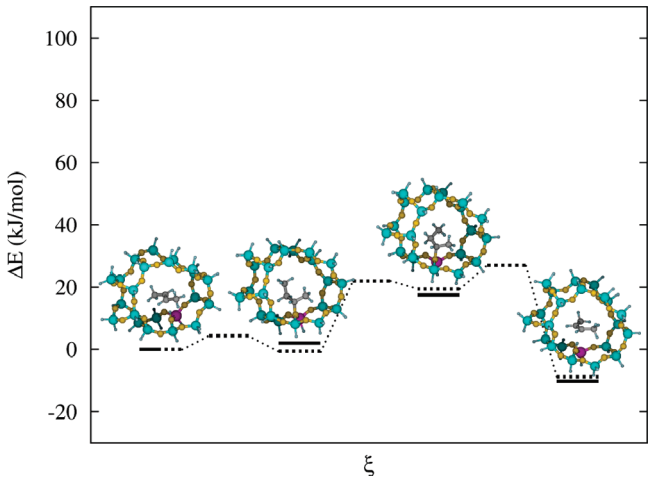

Figure 3. Catalytic pathway for the but-2-ene isomerization in the 22T H-ZSM-5 system and optimized ground-state HLBs minima: from the left, the reactants (*Ad-trans* and *Ad-cis*) and the intermediates (*In-trans* and *In-cis*) are shown. The *Ad-cis* species is the most stable fragment in the path: in the LLBs calculation, dotted bars, $E_0 = -8712.9048$ au, in the HLBs calculation, solid bars, $E_0 = -8755.9702$ au. Following the relative stability of the but-2-ene isomers inside the H-ZSM-5 fragment, the reaction coordinate, ξ, goes from the left to the right.

but-2-ene $^3(\pi\pi^*)$ state by ca. 300 kJ/mol. Hence, identifying the TS occurring in the *in vacuo cis*- to *trans*-but-2-ene isomerization with states like the relatively more stable $^3(\pi\pi^*)$, having the C2-C3 rotated by 90°, we can rationalize the found low interconversion speed by the high activation energies characterizing the involved TS.

3.4. Catalyzed But-2-ene Isomerization. *3.4.1. Unsupported H-ZSM-5 Fragment.* The *cis*/*trans* but-2-ene isomerization was simulated within the H-ZSM-5 cavity shown in Figure 1a. At variance with the π-bonded *cis*- and *trans*-but-2-ene, in the structures of the intermediates (*In-trans* and *In-cis*) and transition states (TS0, TS1, TS2, and TS3) the zeolite acidic hydrogen binds (moves toward) one of the carbon atoms -- by convention C3 -- involved in the alkene bond, reducing the double to a single bond, while the other central carbon atom (C2) is bound to one oxygen (usually that originating from the acidic -OH) of the aluminum-modified T moiety. For these reasons the isomer interconversion becomes easier, with respect to the uncatalyzed process, and occurs in the ground state by hydrogen addition−elimination.

Ignoring for the sake of simplicity the reaction step including TS3, a low energy kinetic path for the *cis*/*trans* title isomerization inside the zeolite cavity is shown in Figure 3: besides the *Ad-trans* and *Ad-cis* species, two *In*-states and three TSs, with LLBs energy barriers below 25 kJ/mol, are involved. Clearly, the energy minimum structures and the corresponding differential energetics obtained by the LLBs and the HLBs procedures are very similar to each other.

Interestingly, although the involved relative energies are of the same order of magnitude as those reported by Gleeson,[15] it is remarked here that we have found two reaction mechanisms in agreement with Scheme 1. The first, as the one reported by Gleeson, involves one intermediate and two transition states (TS0 and TS3 ≡ TS2), while the second involves two intermediates and three transition states (TS0, TS1, and TS2).

In the pathway of Figure 3 the nonactivated alkene adsorption processes are not explicitly reported; by including them the number of the involved elementary events would correspond to those reported for the iodine catalyzed process.[27] Noticeably, the iodine and the zeolite catalyzed rotation mechanisms and energetics are very similar, and their activation energy barriers are both significantly lowered, compared to the gas phase. The energy drop in both catalytic mechanisms is mostly related to the (sp^2 to sp^3) character change of the C2-C3 alkene bond. However, the *cis*/*trans* zeolite isomerization process could be more favored, with respect to that catalyzed by iodine, in the absence of catalyst aging caused by the parallel carbonaceous formation on the zeolite surface.[25] Indeed, instead of the activated iodine dissociation implying ca. 75 kJ/mol,[27] the catalytic process on the acidic zeolite starts by the nonactivated alkene adsorption and moreover, due to the confinement effects of the zeolite cavities, the *Ad-cis* becomes more stable (ca. 9 kJ/mol at the LLBs level) than the *Ad-trans* derivative.

3.4.2. Supported Pd_2/H-ZSM-5 Fragment. The consideration of the bifunctional metal supported systems was mainly addressed to analyze the effects of the reduced room inside the zeolite cavity and the influence of the modified local zeolite acidity for the presence of metal atoms.[16,17,45] For this reason also the bare-palladium fragments were considered. The singlet states always resulted in being the most stable in the Pd_2, Pd_2H^+, and Pd_2/H-ZSM-5 systems when adsorbing hydrocarbon species. The Pd_2 and Pd_2/H-ZSM-5 systems if not adsorbing hydrocarbons, in agreement with the data of Moc et al.,[48] conversely resulted in the triplet ground state, whereas the protonated Pd_2H^+ species showed a singlet ground state (for details on zeolites embedding Pd atoms, see the Supporting Information).

As already pointed out, all the species involved in the reaction path showed a singlet ground state: as an example the *Ad-trans* and *Ad-cis* triplet states were less stable than the corresponding singlet state species by ca. 40 and 150 kJ/mol, irrespective of the basis set employed. The quintuplet states were also less stable and the corresponding geometries typically lost, as previously observed for the but-2-ene derivatives adsorbed on the Pd_2 and Pd_2H^+ bare fragments, the di-σ adsorption modes shown in the more stable multiplicity states.

The supported zeolite fragment of Figure 1b, obtained by optimizing the Pd_2/H-ZSM-5 system, shows the result of a "reverse spillover" mechanism,[16,17,49,50] namely the diffusion of the acidic hydrogen and its adsorption in between the two Pd atoms. A possible reaction path of the *cis*/*trans* but-2-ene interconversion, mediated by the zeolite cavity embedding the Pd atoms, is shown in Figure 4. Although the direct reaction path, occurring *via* TS3, was not found in the kinetic involving the supported Pd_2/H-ZSM-5 fragment, the mechanism, analogously to what was observed for the unsupported H-ZSM-5 system, besides the nonactivated adsorption events involves two intermediates and three transition states. Furthermore, the optimized HLBs and LLBs ground-state minima show, like in

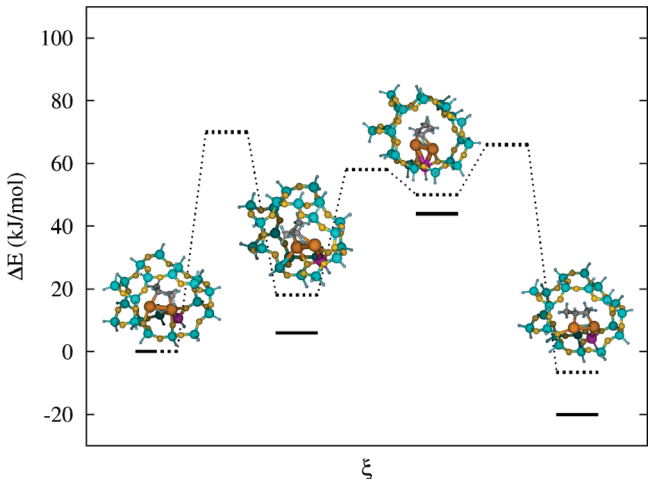

Figure 4. Catalytic pathway for the but-2-ene isomerization in the 22T Pd_2/H-ZSM-5 system and optimized ground-state HLBs minima: from the left, the reactants (*Ad-trans* and *Ad-cis*) and the intermediates (*In-trans* and *In-cis*) are shown. The *Ad-cis* species is the most stable fragment in the path: in the LLBs calculation, dotted bars, $E_0 = -8966.4881$ au, in the HLBs calculation, solid bars, $E_0 = -9009.5066$ au. Following the relative stability of the but-2-ene isomers inside the Pd_2/H-ZSM-5 fragment, the reaction coordinate, ξ, goes from the left to the right.

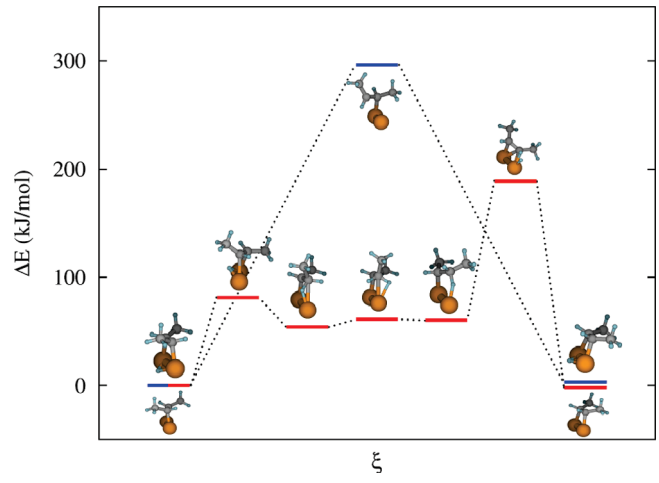

Figure 5. Pathway of the but-2-ene isomerization on bare Pd_2 (blue bars) and Pd_2H^+ (red bars) fragments. The optimized structures of the involved species are shown: down and up bars for the Pd_2 and the Pd_2H^+ processes, respectively. The *Ad-trans* and *Ad-cis* species are the most stable fragments in the Pd_2 ($E_0 = -410.7393$ au) and Pd_2H^+ ($E_0 = -411.0982$ au) reaction path. The reaction coordinate, ξ, from the left to the right follows the process *Ad-trans* → *Ad-cis*.

the unsupported zeolite system, similar geometries and comparable differential energetics (see Figure 4).

Both the *Ad-trans* and *Ad-cis* isomers are adsorbed on the two embedded Pd atoms. Consequently the double bond of the intermediates and transition states is weakened and lengthened, showing a variable extent of sp^2 to sp^3 character change. Of course, the interaction of the C2-C3 alkene group with the hydrogen, bridged between the Pd atoms in the *Ad*-species, promotes the character changes above. Also in this case the adsorbed *cis*-but-2-ene is more stable than the corresponding *trans*-but-2-ene species, by about 6 kJ/mol at the LLBs level, indicating that the reaction, inside the zeolite cavity, could be also favored in the presence of small Pd fragments.

However, the apparent activation energy concerning the formation of TS0, ca. 70 kJ/mol (see Figure 4), is considerably higher than the analogous one observed in the unsupported zeolite cavity (see Figure 3). This higher energy requirement can be rationalized considering the high affinity of the adsorbed hydrogen to the embedded palladium fragment. As a consequence, the acidic hydrogen becomes less available for the addition step, and the isomerization mechanisms inside the supported and unsupported H-ZSM-5 fragments are, to some extent, different.

The effects of the confinement and local acidity on the *cis*/*trans* bifunctional isomerization can be deepened by analyzing Figure 5, which shows the isomerization routes on the bare palladium fragments. Similar diagrams characterizing less favorable processes, not reported here for simplicity, were obtained either considering the species in triplet and quintuplet states and/or considering different but-2-ene derivative adsorption modes (namely, π and mono-σ). Clearly, the presence of one acidic center decreases the activation energies involved in the *cis*/*trans* isomerization when the same occurs on bare palladium. In particular, the protonated palladium fragment process involves equivalent adsorbed reagents, intermediates, and transition states.

Although these resemble the adsorbed hydrocarbon species observed inside the H-ZSM-5 cavity, the corresponding energetics is very different and less favorable to the occurrence of the whole process. This allows us to state that the confinement effects lead to a selective decrease of the activation energy values, mainly produced by the relative destabilization of the different derivatives adsorbed in the zeolite cavities (see also section 3.2). In the Pd_2H^+ system, the adsorbed *cis*-but-2-ene is more stable than the *trans* one, showing that besides the confinement also the local acidity could affect the stability of the adsorbed but-2-ene isomers. The role of the acidic hydrogen is also confirmed by analyzing the process occurring on the unprotonated Pd_2 fragment. In this case the mechanism changes: i) favoring the migration (2→1) of the double bond, ii) involving just one TS, showing a higher activation energy, and iii) leaving the adsorbed *trans* species more stable than the *cis* isomer.

Further considerations, being aware of the intrinsic limits of the approach, deserve the analysis of the Mulliken charges on the carbon atoms of the different but-2-ene derivatives. In Table 3 are reported the average values between topologically equivalent *cis* and *trans* carbon atoms for the different derivatives (e.g., C_4H_8) in the different definition environment (e.g., isolated), as determined by the LLBs approach. From the table, it appears that the terminal carbons (C1 and C4) are not affected by the isomerization steps. Other regular behavior is i) the increased negative charge on the C3 carbon atoms (especially in the *In* and TS species), caused by the interaction of the alkene with either the supported or the unsupported zeolite cavity surface, and ii) the values of the negative charges in the, free to rotate, -$C3H_2$-group, which in the *In* and TS species are higher than those of the fixed -$C2H_2$-group and approach the charge characterizing the terminal CH_3-group. Finally, the inversion of the charge sign

Table 3. Average Mulliken Charges of But-2-ene Species Involved in *Cis*/*Trans* Isomerization

but-2-ene derivative[a]	C1	C2[b]	C3	C4
C_4H_8	−0.35	−0.06	−0.06	−0.35
Ad(C_4H_8/H-ZSM-5)	−0.36	−0.16	−0.10	−0.38
In(C_4H_8/H-ZSM-5)	−0.33	0.13	−0.23	−0.35
TS(C_4H_8/H-ZSM-5)	−0.32	0.12	−0.24	−0.34
Ad(C_4H_8/Pd_2/H-ZSM-5)	−0.35	−0.11	−0.12	−0.33
In(C_4H_8/Pd_2/H-ZSM-5)	−0.34	−0.12	−0.21	−0.33
TS(C_4H_8/Pd_2/H-ZSM-5)	−0.34	−0.10	−0.21	−0.31

[a] In the single but-2-ene derivatives the *cis* and *trans* species show very similar Mulliken charges for carbon atoms of a given topological arrangement, irrespective of the definition environment -- i.e. isolated (C_4H_8), inside unsupported zeolite cavity (C_4H_8/H-ZSM-5), and inside supported zeolite cavity (C_4H_8/Pd_2/H-ZSM-5) -- and of the nature of the derivatives -- i.e. *Ad*, *In*, and TS. In the table are reported the average values between the *cis* and *trans* Cn, $n = 1-4$, carbon atoms for the different derivatives in the different definition environment. [b] In the C_4H_8/H-ZSM-5 systems, C2 corresponds to the carbon atom that in the TS and *In* species is bound to one O of the aluminum-modified T environment. In the C_4H_8/Pd_2/H-ZSM-5 systems, C2 is topologically not changed, with respect to the unsupported zeolite systems, after the Pd_2 addition.

in the *Ad* and TS species, involved in the isomerization inside the unsupported zeolite, has to be underlined.

Therefore, if i) the increase of the negative charge on the C2-C3 fragment is related to the sp^2 to sp^3 character change of the corresponding carbon atoms and ii) the inversion of the charge sign on the C2 atom is related to the appearing on it of carbenium character, it is possible to confirm the interpretation given, analyzing the reaction paths of Figures 3 and 4, and to state that the reaction mechanism is strictly connected to subtle changes in the confinement effects of the reaction environment and in the case of bifunctional metal-zeolite catalysts to the latter and to the mutual influence occurring between metallic centers and *BASs*.[45]

4. Conclusions

The preferential binding sites of one or more Pd atoms within a zeolite cavity are the -OH acidic groups surrounding the Al atoms. An interesting related phenomenon is represented by the reverse hydrogen spillover from the zeolite fragment and the corresponding hydrogen binding to the adsorbed Pd atoms, forming hydride species. This local transformation explains the role of the adsorbed Pd fragments on the apparent decrease of the acidic strength of the aluminum-modified zeolites and the related effects on the supported and unsupported H-ZSM-5 catalytic activity.

Concerning the *cis*-but-2-ene ⇄ *trans*-but-2-ene isomerization, such a reaction is very unlikely to occur in the absence of catalytic conditions, because in this case the reaction involves excited intermediate states, implicating the alkene double-bond breaking. On the other hand, the *cis*/*trans* isomerization proceeds within the H-ZSM-5 zeolite cavity because the excited-state energy required for the *in vacuo* reaction is replaced by lower ground-state activation energies, characterizing both intermediates and transition states. The *trans*-but-2-ene → *cis*-but-2-ene process could also be favored, the latter being more stable than the former inside the zeolite cavity. The findings above clearly open new perspectives in understanding catalysis of hydrocarbons with olefins as intermediates. In fact, *cis*/*trans* pathways inside zeolites have been actually hypothesized, in several catalytic reactions implying hydrocarbons, but at variance with the reported energetics here they were up till now neglected due to the involved gas phase thermodynamics.

In the zeolite catalyzed process, the *trans*- and *cis*-but-2-ene/H-ZSM-5 species present π interactions of the but-2-ene double bond with the acidic hydrogen of the zeolite. Conversely, in the structures of the intermediates and transition states, the but-2-ene double bond is reduced to a single bond. Then, one of the originally sp^2 carbons is linked to one oxygen of the aluminum-modified T environment, showing carbenium character, while the other, showing a different extent of sp^3 character, does not chemically interact with the zeolite inner surface.

The *cis*/*trans* title isomerization also occurs within the 22T H-ZSM-5 zeolite fragment in the presence of adsorbed palladium atoms. However, in this case, the intermediates and transition states show higher energy than that characterizing the corresponding species observed in the unsupported zeolite. In particular, the higher activation energy values characterizing the Pd_2/H-ZSM-5 fragment derivatives should be mainly caused by the very high affinity of the acidic hydrogen toward the same metallic centers. The suggested kinetic path on the Pd_2/H-ZSM-5 involves again two intermediates and three transition states. However, despite the fact that the *cis*-but-2-ene isomer inside the zeolite cavity embedding the palladium atoms is, as in the case of the unsupported zeolite, the most stable isomer, the isomerization mechanism in supported and unsupported zeolite appears to be different.

Acknowledgment. This work was supported by the NANOCAT Project, funded in the framework of the 6th Framework Programme of the European Community -- Contract No. NMP3-CT-2005-506621, by the University of Palermo, and by the Italian Ministero dell'Universita e della Ricerca.

Supporting Information Available: The influence of different basis sets employed to study the title reaction; the aggregation sites of the palladium atoms inside the zeolite cavity; and the multiplicity states of the supported systems. This material is available free of charge via the Internet at http://pubs.acs.org.

References

(1) (a) Boudart, M.; Djega-Mariadassou, G. *Kinetics of Heterogeneous Catalytic Reactions*; Princeton U. Press: Princeton, NJ, 1984; pp 38−76. (b) Dumesic, J. A.; Rudd, D. F.; Aparicio, L. M.; Rekoske, J. E.; Trevino, A. A. *The Microkinetics of Heterogeneous Catalysis*; ACS Professional Reference Book: Washington, DC, 1993; pp 1−72. (c) Averill, B. A.; Rietjens, I. M. C. M.; van Leeuwen, P. W. N. M.; van Santen, R. A. In *Catalysis: An Integrated Approach*, 2nd ed.; van Santen, R. A., van Leeuwen, P. W. N. M., Moulijn, J. A., Averill, B. A., Eds.; Elsevier: Amsterdam, 1999; Vol. 123, Chapter 4, pp 109−206. (d) van Santen, R. A.; Neurock, M. *Molecular Heterogeneous Catalysis*; Wiley-VCH: Weinheim, 2006; pp 19−82.

(2) (a) Sauer, J. *Chem. Rev.* **1989**, *89*, 199–255. (b) van Santen, R. A.; Kramer, G. J. *Chem. Rev.* **1995**, *95*, 637–660. (c) Brändle, M.; Sauer, J. *J. Am. Chem. Soc.* **1998**, *120*, 1556–1570.

(3) Miyamoto, A.; Kobayashi, Y.; Elanany, M.; Tsuboi, H.; Koyama, M.; Endou, A.; Takaba, H.; Kubo, M.; Del Carpio, C.; Selvam, P. *Microporous Mesoporous Mater.* **2007**, *101*, 324–333.

(4) (a) Corma, A. *Chem. Rev.* **1995**, *95*, 559–614. (b) Tao, Y.; Kanoh, H.; Abrams, L.; Kaneko, K. *Chem. Rev.* **2006**, *106*, 896–910.

(5) Delahay, G.; Coq, B. In *Zeolites for Cleaner Technologies*; Guisnet, M., Gilson, J.-P., Eds.; Imperial College Press: London, 2002; Vol. 3,Chapter 16, pp 345−374.

(6) (a) Moscou, L. In *Introduction to Zeolite Science and Practice*; van Bekkum, H., Flanigen, E. M., Jansen, J. C., Eds.; Elsevier: Amsterdam, 1991; Vol. 58, Chapter 1, pp 1−12. (b) Corma, A.; Orchillés, A. V. *Microporous Mesoporous Mater.* **2000**, *35*−*36*, 21–30.

(7) (a) Damin, A.; Bonino, F.; Ricchiardi, G.; Bordiga, S.; Zecchina, A.; Lamberti, C. *J. Phys. Chem. B* **2002**, *106*, 7524–7526. (b) Boronat, M.; Concepción, P.; Corma, A.; Renz, M.; Valencia, S. *J. Catal.* **2005**, *234*, 111–118.

(8) Wang, H.; Turner, E. A.; Huang, Y. *J. Phys. Chem. B* **2006**, *110*, 8240–8249.

(9) Demuth, T.; Rozanska, X.; Benco, L.; Hafner, J.; van Santen, R. A.; Toulhoat, H. *J. Catal.* **2003**, *214*, 68–77.

(10) Nieminen, V.; Sierka, M.; Murzin, D. Y.; Sauer, J. *J. Catal.* **2005**, *231*, 393–404.

(11) Tuma, C.; Sauer, J. *Phys. Chem. Chem. Phys.* **2006**, *8*, 3955–3965.

(12) (a) Kazansky, V. B.; Frash, M. V.; van Santen, R. A. *Catal. Lett.* **1997**, *48*, 61–67. (b) Kazansky, V. B. *Catal. Today* **1999**, *51*, 419–434. (c) Sommer, J.; Jost, R. *Pure Appl. Chem.* **2000**, *72*, 2309–2318. (d) Truitt, M. J.; Toporek, S. S.; Rovira-Truitt, R.; White, J. L. *J. Am. Chem. Soc.* **2006**, *128*, 1847–1852.

(13) Milas, I.; Nascimento, M. A. C. *Chem. Phys. Lett.* **2006**, *418*, 368–372.

(14) (a) Xu, T.; Barich, D. H.; Goguen, P. W.; Song, W.; Wang, Z.; Nicholas, J. B.; Haw, J. F. *J. Am. Chem. Soc.* **1998**, *120*, 4025–4026. (b) Wang, X.; Carabineiro, H.; Lemos, F.; Lemos, M. A. N. D. A.; Ramoa Ribeiro, F. *J. Mol. Catal. A: Chem.* **2004**, *216*, 131–137. (c) Boronat, M.; Viruela, P. M.; Corma, A. *J. Am. Chem. Soc.* **2004**, *126*, 3300–3309.

(15) Gleeson, D. *J. Comput.-Aided Mol. Des.* **2008**, *22*, 579–585.

(16) Vayssilov, G. N.; Rösch, N. *Phys. Chem. Chem. Phys.* **2005**, *7*, 4019–4026.

(17) Ivanova Shor, E. A.; Nasluzov, V. A.; Shor, A. M.; Vayssilov, G. N.; Rösch, N. *J. Phys. Chem. C* **2007**, *111*, 12340–12351.

(18) (a) Teunissen, E. H.; van Santen, R. A.; Jansen, A. P.; van Duijneveldt, F. B. *J. Phys. Chem.* **1993**, *97*, 203–210. (b) Sauer, J.; Ugliengo, P.; Garrone, E.; Saunders, V. R. *Chem. Rev.* **1994**, *94*, 2095–2160. (c) Teunissen, E. H.; Jansen, A. P.; van Santen, R. A. *J. Phys. Chem.* **1995**, *99*, 1873–1879. (d) Ivanova Shor, E. A.; Shor, A. M.; Nasluzov, V. A.; Vayssilov, G. N.; Rösch, N. *J. Chem. Theory Comput.* **2005**, *1*, 459–471.

(19) Barone, G.; Casella, G.; Giuffrida, S.; Duca, D. *J. Phys. Chem. C* **2007**, *111*, 13033–13043.

(20) (a) Solans-Monfort, X.; Sodupe, M.; Branchadell, V.; Sauer, J.; Orlo, R.; Ugliengo, P. *J. Phys. Chem. B* **2005**, *109*, 3539–3545. (b) Rozanska, X. X.; Barbosa, L. A. M. M.; van Santen, R. A. *J. Phys. Chem. B* **2005**, *109*, 2203–2211. (c) Jansang, B.; Nanok, T.; Limtrakul, J. *J. Mol. Catal. A: Chem.* **2007**, *264*, 26433–26439.

(21) Milas, I.; Nascimento, M. A. C. *Chem. Phys. Lett.* **2003**, *373*, 379–384.

(22) Wei, J.; Prater, C. D. *Adv. Catal.* **1962**, *13*, 203–392.

(23) Ivanov, P.; Papp, V. *Appl. Surf. Sci.* **2001**, *179*, 234–239.

(24) Nkosi, B.; Ng, F. T. T.; Rempel, G. L. *Appl. Catal., A* **1997**, *158*, 225–241.

(25) de Ménorval, B.; Ayrault, P.; Gnep, N. S.; Guisnet, V. *Appl. Catal., A* **2006**, *304*, 1–13.

(26) (a) Cundall, R. B.; Griffiths, P. A. *Discuss. Faraday Soc.* **1963**, *36*, 111–123. (b) Cundall, R. B.; Griffiths, P. A. *J. Am. Chem. Soc.* **1963**, *85*, 1211–1212. (c) Back, M. H.; Cvetanović, R. J. *Can. J. Chem.* **1963**, *41*, 1396–1406. (d) Back, M. H.; Cvetanović, R. J. *Can. J. Chem.* **1963**, *41*, 1406–1412. (e) Golden, D. M.; Egger, K. W.; Benson, S. W. *J. Am. Chem. Soc.* **1964**, *86*, 5416–5420. (f) Egger, K. W.; Golden, D. M.; Benson, S. W. *J. Am. Chem. Soc.* **1964**, *86*, 5420–5424. (g) Benson, S. W.; Egger, K. W.; Golden, D. M. *J. Am. Chem. Soc.* **1965**, *87*, 468–476.

(27) Kotz, J. C.; Treichel, P. M.; Weaver, G. C. *Chemistry and Chemical Reactivity*, 6th ed.; Thomson Learning: Philadelphia, 2006; pp 729−731.

(28) Delbecq, F.; Zaera, F. *J. Am. Chem. Soc.* **2008**, *130*, 14924–14925.

(29) Cano, M. L.; Hamilton, D. M., Jr.; Thomason, T. B. Production of 1-Alkenes from Mixed Olefin Streams using Catalytic Distillation, U.S. Patent 7355087, 2005.

(30) van Santen, R. A. *J. Mol. Catal. A: Chem.* **1997**, *115*, 405–419.

(31) (a) Baerlocher, C.; Meyer, W. M.; Olson, D. H. *Atlas of Zeolite Framework Types*, 5th ed.; Elsevier: Amsterdam, 2001. (b) *Database of Zeolite Structures*. http://www.iza-structure.org/databases/ (accessed Aug 1, 2008). (c) *Database of Zeolite Structures, Zeolite Framework Types*. http://izasc.ethz.ch/fmi/xsl/IZA-SC/ft.xsl (accessed Nov 5, 2007).

(32) The employed notation follows the topological nomenclature of the MFI framework structure;[31] the first and the second T are coincident with the Al and the Si center, respectively.

(33) Frisch, M. J.; Trucks, G. W.; Schlegel, H. B.; Scuseria, G. E.; Robb, M. A.; Cheeseman, J. R.; Montgomery, J. A., Jr.; Vreven, T.; Kudin, K. N.; Burant, J. C.; Millam, J. M.; Iyengar, S. S.; Tomasi, J.; Barone, V.; Mennucci, B.; Cossi, M.; Scalmani, G.; Rega, N.; Petersson, G. A.; Nakatsuji, H.; Hada, M.; Ehara, M.; Toyota, K.; Fukuda, R.; Hasegawa, J.; Ishida, M.; Nakajima, T.; Honda, Y.; Kitao, O.; Nakai, H.; Klene, M.; Li, X.; Knox, J. E.; Hratchian, H. P.; Cross, J. B.; Bakken, V.; Adamo, C.; Jaramillo, J.; Gomperts, R.; Stratmann, R. E.; Yazyev, O.; Austin, A. J.; Cammi, R.; Pomelli, C.; Ochterski, J. W.; Ayala, P. Y.; Morokuma, K.; Voth, G. A.; Salvador, P.; Dannenberg, J. J.; Zakrzewski, V. G.; Dapprich, S.; Daniels, A. D.; Strain, M. C.; Farkas, O.; Malick, D. K.; Rabuck, A. D.; Raghavachari, K.; Foresman, J. B.; Ortiz, J. V.; Cui, Q.; Baboul, A. G.; Clifford, S.; Cioslowski, J.; Stefanov, B. B.; Liu, G.; Liashenko, A.; Piskorz, P.; Komáromi, I.; Martin, R. L.; Fox, D. J.; Keith, T.; Al-Laham, M. A.; Peng, C. Y.; Nanayakkara, A.; Challacombe, M.; Gill, P. M. W.; Johnson, B.; Chen, W.; Wong, M. W.; Gonzalez, C.; Pople,

J. A. *Gaussian 03, Revision D.02*; Gaussian, Inc.: Wallingford, CT, 2005.

(34) (a) Becke, A. D. *J. Chem. Phys.* **1993**, *98*, 5648–5652. (b) Stephens, P. J.; Devlin, J. F.; Chabalowsky, C. F.; Frisch, M. J. *J. Phys. Chem.* **1994**, *98*, 11623–11627.

(35) Tirado-Rives, J.; Jorgensen, W. L. *J. Chem. Theory Comput.* **2008**, *4*, 297–306.

(36) Stratmann, R. E.; Scuseria, G. E.; Frisch, M. J. *J. Chem. Phys.* **1998**, *109*, 8218–8224.

(37) (a) Schreiner, P. R. *J. Am. Chem. Soc.* **1998**, *120*, 4184–4190. (b) Cramer, C. J. *J. Am. Chem. Soc.* **1998**, *120*, 6261–6269. (c) Schreiner, P. R.; Prall, M. *J. Am. Chem. Soc.* **1999**, *121*, 8615–8627. (d) Clark, A. E.; Davidson, E. R.; Zaleski, J. M. *J. Am. Chem. Soc.* **2001**, *123*, 2650–2657. (e) Graefenstein, J.; Kraka, E.; Filatov, M.; Cremer, D. *Int. J. Mol. Sci.* **2002**, *3*, 360–394.

(38) Hariharan, P. C.; Pople, J. A. *Theor. Chim. Acta* **1973**, *28*, 213–222. (b) Francl, M. M.; Petro, W. J.; Hehre, W. J.; Binkley, J. S.; Gordon, D. J.; De Frees, M. S.; Pople, J. A. *J. Chem. Phys.* **1982**, *77*, 3654–3665.

(39) (a) Binkley, J. S.; Pople, J. A.; Hehre, W. J. *J. Am. Chem. Soc.* **1980**, *102*, 939–947. (b) Gordon, M. S.; Binkley, J. S.; Pople, J. A.; Pietro, W. J.; Hehre, W. J. *J. Am. Chem. Soc.* **1982**, *104*, 2797–2803.

(40) Hay, P. J.; Wadt, W. R. *J. Chem. Phys.* **1985**, *82*, 270–283.

(41) Raghavachari, K.; Trucks, G. W. *J. Chem. Phys.* **1989**, *91*, 1062–1065.

(42) Foresman, J. B.; Frisch, Æ. *Exploring Chemistry with Electronic Structure Methods*, 2nd ed.; Gaussian Inc.: Pittsburgh, PA, 1996; pp 61−90.

(43) Peng, C.; Ayala, P. Y.; Schlegel, H. B.; Frisch, M. J. *J. Comput. Chem.* **1996**, *17*, 49–56.

(44) Boys, S. F.; Bernardi, F. *Mol. Phys.* **1970**, *19*, 553–566.

(45) Kubicka, D.; Kumar, N.; Venäläinen, T.; Karhu, H.; Kubickova, I.; Österholm, H.; Murzin, D. Yu. *J. Phys. Chem. B* **2006**, *110*, 4937–4946.

(46) Yoda, E.; Kondo, J. N.; Domen, K. *J. Phys. Chem. B* **2005**, *109*, 1464–1472.

(47) Roos, B. O. In *Computational Photochemistry*; Olivucci, M., Ed.; Elsevier: Amsterdam, 2005; Vol. 16, Chapter 10, pp 317−348.

(48) Moc, J.; Musaev, D. G.; Morokuma, K. *J. Phys. Chem. A* **2008**, *112*, 5973–5983.

(49) Conner, W. C., Jr.; Falconer, J. L. *Chem. Rev.* **1995**, *95*, 759–788.

(50) Bowker, M.; Bowker, L. J.; Bennett, R. A.; Stone, P.; Ramirez-Cuesta, A. *J. Mol. Catal. A: Chem.* **2000**, *163*, 221–232.

CT800402K